6

A SEARCH FOR MAGNETISM IN PT ATOMIC CHAINS USING SHOT NOISE

Manohar KUMAR, Alexander SMOGUNOV, Oren TAL, Roel H.M.SMIT, Erio TOSATTI, Jan van RUITENBEEK

Pt is known to show spontaneous formation of chains of metal atoms upon breaking a metallic contact. From model calculations these have been suggested to become spin polarized, which is related to the Stoner enhanced susceptibility of bulk Pt and the increased density of states due to the reduced dimensionality. Here, we use shot noise measurements to search for evidence on the magnetic state of Pt atomic chains. We find evidence for a non-magnetic ground state for the conductance channels of Pt atomic chains. This may imply that the magnetic splitting of the conductance channels in Pt atomic chains is too small for detection via shot noise, that our chains are not long enough for the magnetic order to fully develop. Surprisingly, we find many atomic chains that have just two conductance channels, for which one has a full transmission of $\tau \simeq 1$.

This chapter is submitted to Phys. Rev. B.

6.1 MOTIVATION: ITINERANT MAGNETISM IN PT ATOMIC CONTACTS

AT nanometer size scales one often finds unexpected behavior of matter. A particularly appealing example is the spontaneous formation of chains of metal atoms upon breaking a metallic contact [1–3]. Pt is a metal with a modestly Stoner-enhanced magnetic susceptibility, indicating proximity to a ferromagnetic state. A transition to ferromagnetism can be induced by an increase in the density of states due to Van hove band edge singularities at the Fermi level. This can bring the system beyond the Stoner limit, e.g. by reduction of dimensions, as evidenced by recent work on Pt clusters of 10 atoms [4]. This makes it likely that for purely 1D systems magnetism may also develop, i.e. for atomic chains. Regarding long-range order the Leib-Mattis theorem predicts that the ground state of the 1-D system should be non magnetic. However, local magnetic order in an atomic chain of finite length suspended between the two bulk metal leads could still develop. Moreover, a large magnetic anisotropy energy barrier makes magnetic state as ground state of 1-D system feasible [5]. For these reasons, the ferromagnetic order predicted from model calculations for atomic chains [6–10] was not fully unexpected. Remarkable features for Pt atomic chains are the fact that the Stoner instability is expected close to the equilibrium lattice spacing, and that it becomes more pronounced with increase in chain length [7]. The obvious question is how to obtain experimental evidence for this induced local moment magnetism in the Pt monatomic chains. For Pt atom contacts an advantage is the fact that the leads are paramagnetic and that any evolution of magnetism can be safely attributed to the point contact. Here, we exploit shot noise, the intrinsic noise due to the discrete character of the electronic charge, for revealing information on the magnetic state of Pt atomic chains. We find evidence for a non-magnetic ground state of the conductance channels for Pt atomic chains in our experiments.

6.2 FORMATION OF PT ATOMIC CHAINS

FORMATION of platinum atomic junctions was done at liquid helium temperatures using mechanically controllable break junctions (MCBJ) [11, 12]. The electronic circuit for the measurement is shown schematically in figure (3.5). The sample chamber was pumped to $\sim 10^{-5}$mbar before cooling down in liquid helium. The chamber was fitted with active charcoal for cryogenic pumping such that the pressure in the chamber drops below measurable values at liquid He temperature. Once cold and under vacuum the Pt sample wire was first broken by mechanical bending of the substrate. By relaxing the bending the broken wire ends can be rejoined and the size of the contact can be adjusted with sub-atomic preci-

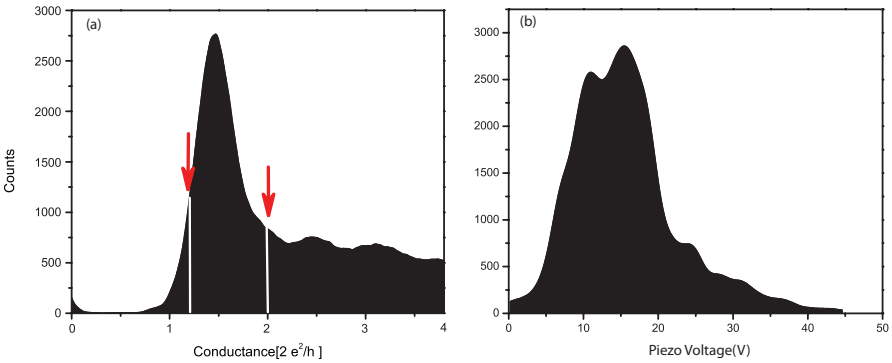

FIGURE 6.1: DC characterization of Pt atomic contacts: (a) Conductance histogram for a clean Pt contact at liquid helium temperatures. Histogram made from 1000 conductance traces. The peak at $1.5G_0$ shows the typical conductance of the clean Pt atomic contact. (b) Corresponding length histogram recorded for a Pt break junction, by recording the lengths of the conductance traces between the boundaries shown by the red arrows in (a).

sion by means of a piezo-electric actuator.

6.2.1 DC CHARACTERIZATION

Before starting shot noise measurements the Pt contact was first characterized by recording a conductance histogram, figure (6.1 a). The conductance histogram for a clean Pt contact at liquid helium temperatures is recorded by combining one thousand conductance breaking traces. Contacts are repeatedly made and broken, controlled by the piezo voltage that regulates the substrate bending of the mechanically controllable break junction device, at a fixed bias voltage setting of 80mV. The points of the digitized traces of conductance are collected into a histogram and the counts are plotted as a function of the conductance. The first peak at $\sim 1.5\cdot(2e^2/h)$ represents the average conductance of a contact of a single Pt atom in cross section. Below this peak the count drops to very low numbers, indicating that the contact finally breaks to a clean vacuum tunnel junction. Note that we use units[1] of $2e^2/h$ here for reasons of comparing to earlier work, but that the conductance units per spin, e^2/h, are used throughout the text in this chapter. The arrows indicate the boundaries used for recording length histograms as in figure (6.1 b). Figure (6.1 b) shows a length histogram obtained for a clean Pt junction at low temperatures. This is used to verify chain formation and for calibrating the displacement. The histogram in figure (6.1 b) is obtained by combining 4500 traces and recording the length of the conductance plateaux with conductances between

[1] $1G_0 = 2e^2/h$

1.2 and 2 times ($2e^2/h$), *i.e.* in the range of the first conductance peak between the red arrows in figure (6.1 a). The length axis is given in units of the voltage on the piezo element, where the proportionality constant is 2.5 V/Å. The histogram is consistent with the earlier work of Untiedt *et al.*[1]. The first three peaks can be interpreted as the lengths corresponding to chains of 2, 3, and 4 atoms.

6.2.2 AC CHARACTERIZATION

Differential conductance spectra were measured by means of a small modulation voltage (2mV and 2.3kHz) and a lock-in amplifier. Typical differential conductance traces measured on Pt atomic contacts of several lengths are shown in figure (6.2). The differential conductance traces have predominantly zero bias anomalies in the form of a Kondo-like dip, a Kondo-like peak or split peak features. The zero bias anomalies seen here for Pt atomic contacts are similar to what has been seen for ferromagnetic atomic contacts (see figures (7.4, 7.5)). In a few cases clear step features have been seen that could be attributed to the inelastic electron-phonon interaction, similar to the inelastic features seen in case of Au atomic contacts, see section 4.2.2.

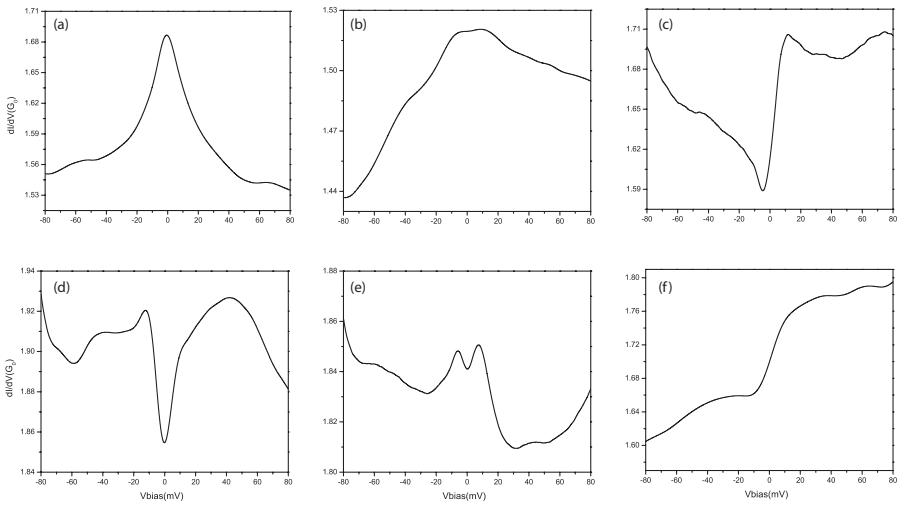

FIGURE 6.2: Differential conductance spectra for Pt atomic contacts: The variation in the differential conductance spectra is quite rich. It shows zero bias peaks, dips, or Fano-like resonances, and step features that may be due to inelastic interaction

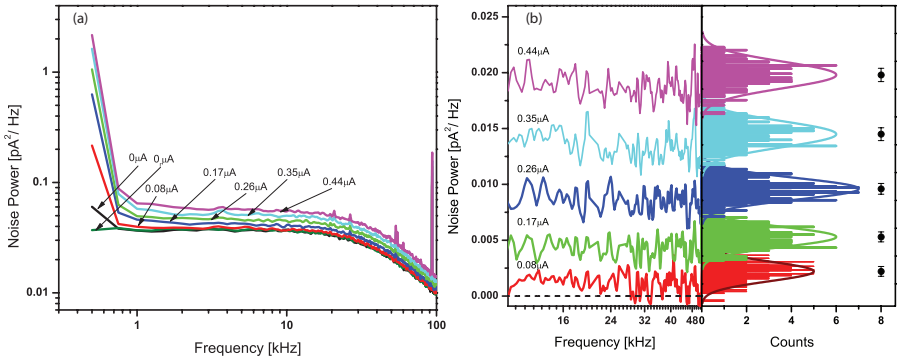

FIGURE 6.3: An example of the noise power data analysis. (a) Noise power spectra for a Pt atomic chain of ~ 3 atoms in length having a conductance $G = 1.52 \cdot (2e^2/h)$ and a Fano factor F=0.192. The peaks are due to spurious signals that could not be fully shielded. (b) Same data after subtracting the thermal noise and correcting for the roll-off. The spurious signals are effectively removed by the subtraction procedure.

6.3 SHOT NOISE SPECTROSCOPY

SHOT noise was measured by using two sets of low-noise amplifiers, with a total amplification factor of 10^5, and by taking the cross spectrum of the two channels in a frequency range between 250Hz and 100kHz. After averaging of 10^4 spectra the uncorrelated noise of the preamplifiers is strongly suppressed. During the shot noise measurements the conductance circuit was disconnected in order to eliminate external noise sources. An example of noise spectra for a series of current settings is given in figure (6.3), which illustrates how the noise power is obtained from the data. The spectra are flat in the middle but at the low-frequency end one observes an increase above the white noise level due to a $1/f$-like noise contribution. The amplitude of this feature varies between different junction settings, and it has been attributed to defect fluctuations in the leads [13]. This part of the spectrum is ignored for the analysis, but it influences the accuracy of the determination of the white noise power. At the high-frequency end of the spectrum a roll-off is seen, with a characteristic frequency of about 50kHz that is due to the RC time constant of the stray capacitance of the leads in combination with the junction resistance. Finally, a slight upturn in the spectra at the highest frequencies is due to residual correlations in the noise of the two amplifiers. The analysis presented below eliminates the roll-off, but is sensitive to the residual correlations and the $1/f$ noise, which limit the accuracy in determination of the Fano factor.

After the initial characterization of the junction an atomic chain was made by pulling, starting from a large contact until the conductance dropped to a value

near $1.8 \cdot (2e^2/h)$. Measurements of conductance and noise were taken at several points of subsequent stretching starting from here. The corresponding piezo voltages were recorded in order to identify the length in terms of the mean number of atoms forming the chain. The zero-bias differential conductance, dI/dV, was recorded, which is needed in combination with the noise for the analysis of the conductance channels. The accuracy of the ac conductance measurement is better than 1%, as verified by tests on standard resistors. First, the thermal noise is recorded at zero bias, and after taking noise spectra at several bias settings the zero bias noise is recorded once more (labeled as $0_r\,\mu$A) in order to verify that the junction has remained stable. The thermal noise level corresponds to a temperature of 6.3 K, which agrees within the accuracy of the temperature measurement with a reading of 6.1 K, as obtained from a ruthenium oxide 10k resistance thermometer. For several junction settings conductance measurements were repeated after the shot noise bias sequence in order to detect possible changes in the conductance. Typical changes observed were smaller than 2%. Figure (6.3 b) shows that the spectra become white above 10kHz after correction for the roll-off with a single RC time constant. The thermal noise (at zero bias) is subtracted, which explains the negative values in the data fluctuations for the lowest currents. The data points are projected in the form of a histogram, shown at the right, and the level of white noise is obtained from the position of the center of the histogram for each voltage bias. The bullets and error bars at the right indicate the position and accuracy of the noise power as determined from a Gaussian fit to the histograms.

6.4 SHOT NOISE IN A SPIN DEGENERATE CONDUCTOR

THE theory for shot noise is discussed in detail in section (1.3) and the measurement techniques are presented in chapter 2. For a nanoscale conductor with N spin non-degenerate conductance channels, each characterized by a transmission probability τ_n, the current noise power at an applied bias voltage V is given by,[2]

$$S_I = 2eV \coth\left(\frac{eV}{2k_B T}\right) \frac{e^2}{h} \sum_{n=1}^{N} \tau_n(1-\tau_n) + 4k_B T \frac{e^2}{h} \sum_{n=1}^{N} \tau_n^2 \,. \tag{6.1}$$

where k_B is Boltzmann's constant, and T is the temperature of the nanoscale conductor. In equilibrium (at $V = 0$) equation (6.1) reduces to the Johnson-Nyquist thermal noise, $4k_B TG$, describing the current fluctuations that are driven only by the thermal motion of electrons. $G = (e^2/h)\sum \tau_n$ is the conductance. Again, in

[2] Anticipating spin splitting of the conductance channels we treat conductance channels for each spin direction separately. Equation (6.1) is similar to equation (1.23), except that the spin degeneracy of the channels is lifted.

the expression for G we take the conductance quantum as e^2/h and sum over spin states. In the low-temperature limit, $k_B T \ll eV$, equation (6.1) reduces to $S_I = 2e\bar{I}F$, where the Fano factor F measures the quantum suppression of Schottky's classical result,

$$F = \frac{\sum_n \tau_n(1-\tau_n)}{\sum_n \tau_n}. \tag{6.2}$$

From this analysis it is apparent that one may obtain information on the transmission probabilities of the conductance channels by measurement of the noise power, and in favorable cases it is even possible to determine the number of conductance channels [14]. The Fano factor reduces to zero when all conductance channels are either fully blocked ($\tau_n = 0$), or fully open ($\tau_n = 1$). For a nanowire with a given conductance $G = (e^2/h)\sum \tau_n$ the noise has a lower bound that is obtained by taking all open channels to have perfect transmission, except for one that takes the remaining fraction of the conductance. This minimum will sensitively depend on whether the spin channels are restricted to be degenerate. Let us take as an example the case $G = 1.5 \times 2e^2/h$: the minimum Fano factor for the spin degenerate case would be $F = 0.166$, for a channel composition of $\tau_1 = 1$ and $\tau_2 = 0.5$. In case of spin split channels the conductance is written in terms of the transmission probabilities for the spin channels as $3 \times e^2/h$ and the minimum Fano factor is now obtained for all three spin channels completely open, giving $F = 0$. It is this property that we exploit when investigating the magnetic state of Pt atomic chains. This has been elaborated in figure(3.13).

Since shot noise and thermal noise are of comparable magnitude in these experiments it is useful to represent the data such that the expected dependence on the applied bias in equation (6.1) is apparent. The voltage dependence in equation (6.1) can be lumped into a single variable X that we take to be $X = x\coth(x)$, with $x = eV/2k_B T$. We define the reduced excess noise Y as $Y = (S_I(V) - S_I(0))/S_I(0)$, where $S_I(V)$ is the noise at finite bias, and $S_I(0)$ is the thermal noise, at zero bias. The reduced excess noise is now expected to depend linearly on the control parameter X, $Y = (X-1)F$, from which the Fano factor F can be easily obtained (please see section (3.5.3) for details). Figure (6.4) shows a series of measurements on a Pt atomic chain with a conductance of $G = 1.425 \pm 0.01(2e^2/h)$ at a short length of 2 atoms in the chain, for 26 settings of the bias voltage in the range from 0mV to 16.6mV (0 to 1.83μA). The slope of the plot gives a Fano factor $F = 0.269 \pm 0.009$. The accuracy for each of the points is 3%, as obtained by a fit to the power spectrum after correction for the roll-off as in figure (6.3). The measurement required about 50 minutes, illustrating the long-term stability of the atomic chains. It shows a very nice agreement with the expected dependence, and the scatter around the linear slope is within the data point accuracy.

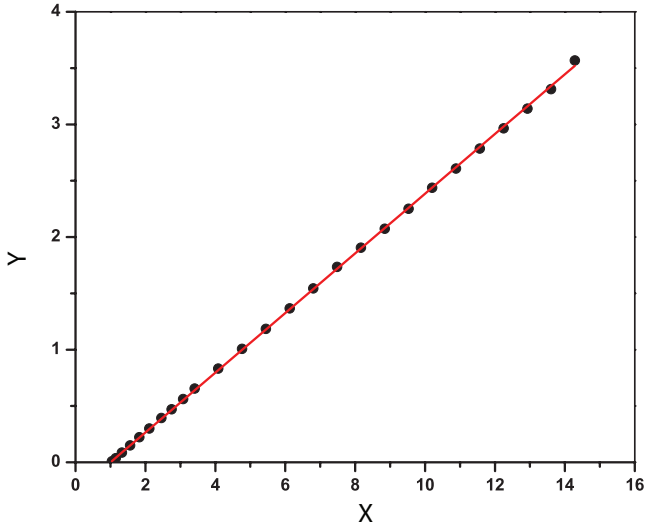

FIGURE 6.4: Reduced excess noise $Y = (S_I(V) - S_I(0))/S_I(0)$ for a Pt atomic chain. The excess noise is given as a function of $X = x\coth(x) = (eV/2k_BT)\coth(eV/2k_BT)$, for a chain having a conductance of $G = 1.425 \pm 0.01(2e^2/h)$ at a length of about 2 atoms in the chain. The slope of the linear fit (solid red line) gives a Fano factor $F = 0.269 \pm 0.009$.

We have recorded similar plots for over 500 configurations of Pt atomic chains of various length, for which we took 7 bias voltage points between 0 and 0.44μA. When the scatter in the plot of the reduced excess noise was larger than 3%, or the thermal noise at start and end of the measurement differed by more than 2%, we rejected the data. The scatter is mostly due to a large $1/f$ component in the noise spectrum and the contribution of the residual amplifier noise correlations to the spectra. After this selection 119 configurations remain. Figure (6.5) shows the Fano factors determined from these 119 sets of shot noise measurements.

The red curve shows the minimum noise curve when spin degeneracy is imposed. Relaxing spin degeneracy results in a minimum noise curve shown by the black curve. The blue broken lines show the *maximum* noise that can be obtained with $N = 4$ or $N = 6$ (spin) channels. This maximum is obtained by taking all channels to have the same transmission probability $\tau = Gh/Ne^2$, leading to $F = 1 - \tau$. The measured data points form a diffuse cloud in (G,F)-space, with its centre of mass near $G = 1.5 \times (2e^2/h)$ and a spread in this conductance in agreement with the position and width of the first peak in the conductance histogram. A large fraction of the points lie above the line labeled $N = 4$, which represents the maximum

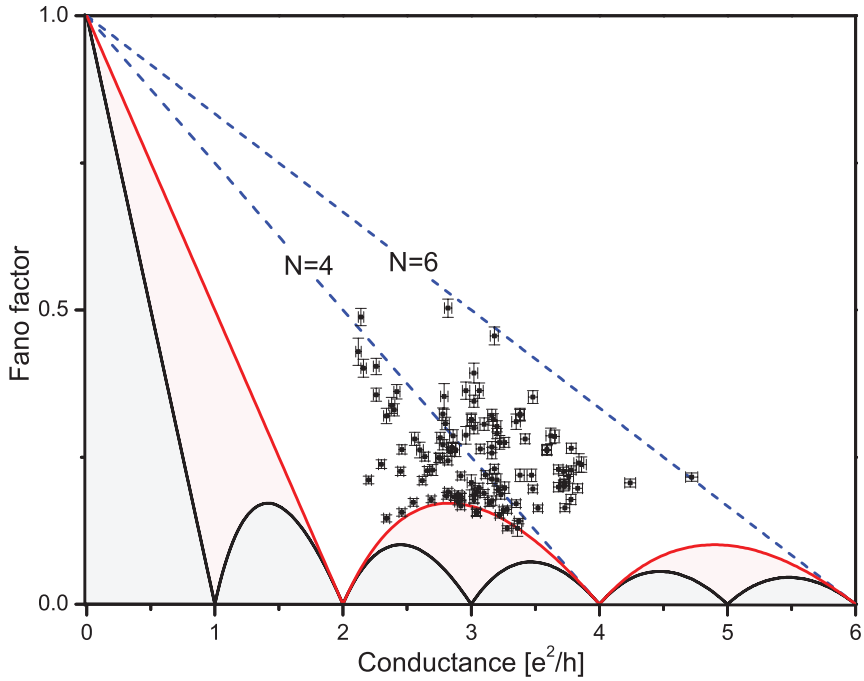

FIGURE 6.5: Fano factor vs. conductance for 119 different Pt atomic chain configurations. The bold red curve shows the minimum noise curve that applies when spin degeneracy is imposed. Relaxing the requirement of spin degeneracy results in a minimum noise curve shown by the thin black curve. The inset illustrates the principle of the break junction experiment.

Fano factor when only four channels are available. This shows that these Pt atomic chains have at least five conductance channels, in agreement with calculations [8, 15, 16]. The points below the blue broken line $N = 4$ can be explained by four channels, but for the majority of points the only conclusion we can draw is that *at least* four channels are involved. The most striking observation, and the central result is that all Fano factors for the Pt chain configurations fall on, or well above, the curve describing the minimum noise for *spin-degenerate* channels. More than 15% of the measured points are even found to coincide within the error bars with the minimum Fano curve for spin-degenerate channels, and none of the points are found significantly below it. For spin-split conductance channels the limiting curve is represented by the black curve in figure (6.5) [17, 18]. This suggests that any possible spin splitting of the conductance channels in the Pt atomic chains formed in the experiment is small, which does not appear to agree with the results

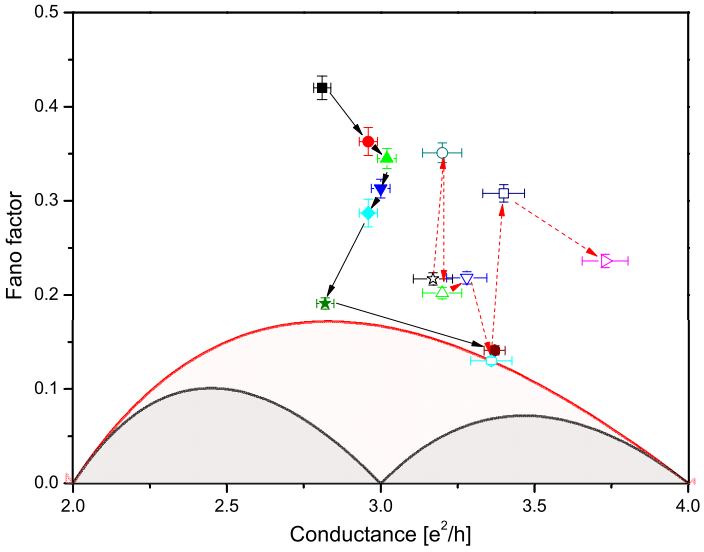

FIGURE 6.6: Fano factor evolution with stretching sequence of the Pt atomic contact. Two examples are shown of the evolution of conductance G and Fano factor F when a Pt atomic chain is stepwise elongated. The stretching sequence has a length of 3.0V on the piezo (~ 12Å, solid arrows and filled symbols) and 3.52V (~ 14Å, dashed arrows and open symbols), corresponding to 5 or 6 atoms final length, respectively. These two examples are chosen to illustrate that there does not appear to be a systematic evolution towards the minimum noise curve for longer chains, although points at the boundary curve are more frequently found for longer chains.

from DFT calculations [6, 8–10, 16]. The most complete calculations [8], fully relativistic Density Functional Theory for realistic chain sizes, show that a magnetic moment above 0.4μB per atom already appears for a chain only three atoms in length, at equilibrium interatomic distance. Most points in figure (6.5) are measured for Pt chains of 3 to 4 atoms in length, occasionally 5 or 6 atoms. We do not find any systematic evolution of the Fano factor with stretching of the chain. While increasing the length of the chain in steps the Fano factor may be seen to jump towards the minimum noise curve, but then it jumps away from the curve to higher values at next steps in increasing the chain length (see figure (6.6)). A second remarkable observation is the fact that there is a group of 18 points that coincide with the curve describing the minimum noise power for spin degenerate channels. All calculations predict that at least six spin channels are involved, [8, 15, 16, 19],

but the transmission probability for each of these channels may be sensitive to the particular arrangements of the atoms at the leads. Pauly *et al.* have presented tight binding model calculations for Pt atomic chains at many stages of stretching of the contact [20]. Their results, that do not include spin polarization, show that frequently the system is found in a configuration with one spin-degenerate channel nearly fully open, while there is only one additional spin-degenerate channel that has significant contribution to the conductance. These configurations may correspond to the ones at the red boundary in figure (6.5).

6.5 THEORY AND DISCUSSION

We wish to evaluate the impact of spontaneous spin polarization of long chain Pt break junctions on their electron transmission, and from that on their shot noise. Spin polarized DFT, including spin orbit interaction,[8, 9], (with the possible addition of self-interaction corrections for d orbitals) constitutes in principle a valid approach to this problem. To be sure, DFT is a mean field theory, ignoring all possible many body Kondo screening effects – generally non negligible at magnetic atomic and molecular contacts.[21]. However in long chains whose overall spin is expected to be large, $S \gg 1/2$, magnetic anisotropy will only allow for two low energy states $\pm S$. In that case, it will be impossible for conduction electrons to cause spin flip, and no Kondo screening and no zero bias anomalies should occur, in agreement with experiment – except possibly for $S = 1/2$, a situation which may be realized in very short contacts.

Moreover, because the calculated energy barrier between states S and $-S$ of the chain is very large[9], we anticipate a blocking temperature safely above 4 K, so that thermal fluctuation effects should also be negligible during the typical short electron traversal time across the contact.

High symmetry Pt chain contact spin polarized DFT calculations showed a large number of channels and a conductance generally above $2G_0$, to be compared with an experimental break junction histogram peak around $1.5G_0$. Spontaneous polarization emerges from 3-atom chains upwards, increasing with chain length and with chain stretching. Somewhat disappointingly however, the predicted dependence of transmission and of ballistic conductance upon the onset of magnetism was only modest. The reason for the relative insensitivity of transmission upon magnetism is that the main electronic state driving magnetism, $|m_j| = 5/2$, has a narrow-band d character, with a small group velocity at the Fermi level, and low or negligible electron transmission. On the other hand, wide-band states with a large group velocity that dominate electron transmission, and thus both conductance and shot noise, possess more s-band admixture and are only modestly spin polarized. As we will see, that insensitivity carries over to shot noise.

Ideally, we would need to calculate transmission, conductance and noise applying the same DFT accuracy of [8] to realistic geometries such as those identified in Ref. [20]. Even without that, we can anticipate that the main effect of reduced symmetry in long chain contacts will again be, as in the tight binding modeling of Pauly *et al.*, to effectively block most channels except four surviving ones. In that case, a qualitative understanding of their spin polarization dependence can be obtained even without explicitly calculating transmissions, by simply studying the conduction channels of the infinite ideal chain. Its simple electronic structure in the end is better suited for qualitative understanding than a specific, cumbersome calculation for long chain contact transmission and noise. The main questions are: what is the level of spin polarization of those chain bands that will lead to surviving channels, and what effect would that magnetism have on noise? Another question is whether the presence of Pt chain magnetism could be endangered by self-interaction errors, that are uncorrected in straight DFT. To clarify first this last point, we conducted DFT calculations, for the infinite ideal Pt chain at its equilibrium spacing of 2.35Å , in three different flavors, namely LSDA, LSDA+U and LSDA+U+J, as implemented in the PWSCF code of Quantum Espresso[22].

As shown in figure (6.7), mitigation of self-interaction errors does lead to a change of magnetism. Addition of a small Hubbard U=1eV for d states is enough to quench magnetism at equilibrium spacing as in (b). However, upon successive addition of a moderate exchange parameter (J = 0.5 eV is a standard value for Pt) the chain reverts back to strong magnetism as shown in (c). This leads us to conclude that the uncertainty connected with self-interactions in DFT, an aspect only rarely addressed so far in this context [23], makes the presence and magnitude of spin polarization hard to predict in a Pt chain contact at zero mechanical strain. Nonetheless, we find that a frank spin polarization is recovered even in the worst case for even moderately stretched chains. A substantial level of strain is generally expected in chains formed by break junctions [20], that should therefore be magnetic. Conductance channels in a long chain nanocontact can be identified by infinite chain bands that cross the Fermi level. For increasing k-vector, there are in all cases six channels: (1±)$m_j = \pm 1/2(d_z^2 + s)$; (2±) $m_j = \pm 3/2(d_{xz}, d_{yz})$; (3±)$m_j = \pm 1/2(s + d_z^2)$. In addition, depending on spontaneous magnetization, additional d channels (4±) $m_j = \pm 3/2$, and (5-) $m_j = -5/2$ may also be open at Fermi. The latter band is poorly dispersive (has a small group velocity) and is largely spin split across Fermi by magnetism, and can be considered the main "actor" band responsible for spontaneous spin polarization. Other bands are "spectators" whose spin splitting is small or irrelevant, while their group velocities at Fermi are larger. Even without a detailed calculation, the circumstances of conduction in Pt chain contacts are now apparent. The fully spin polarized actor channel(s) is easily blocked because of its large mass, and only some of the poorly po-

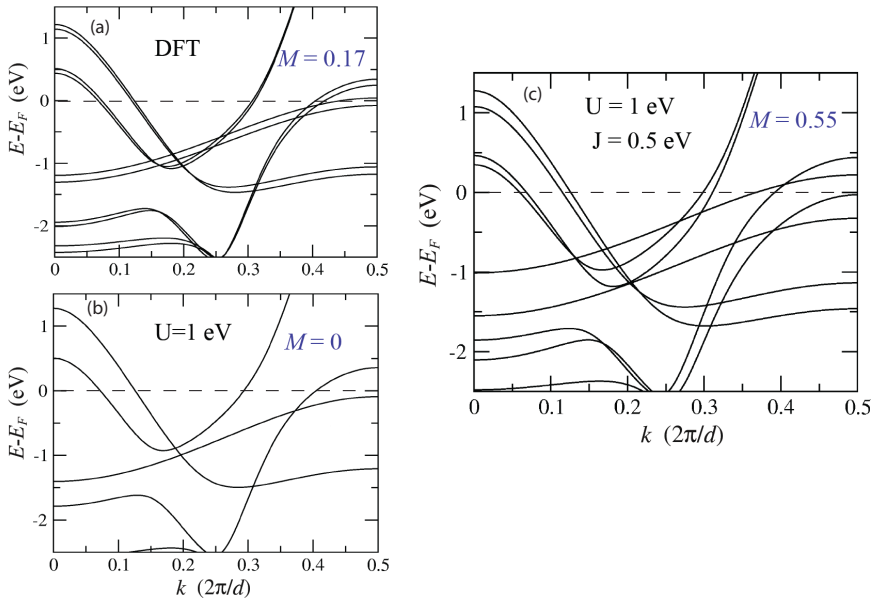

FIGURE 6.7: Electronic structure of an infinite Pt chain at T=0 and at the equilibrium spacing of 2.35Å, calculated by DFT in different approximations, namely: (a) LSDA, yielding a spin moment of $0.17\mu_B$ and an orbital moment of $0.22\mu_B$ per atom; (see [8] for computational details). (b) LSDA + U with $U = 1$ eV, yielding a nonmagnetic ground state. (c) LSDA+U+J, with $U = 1$ eV and $J = 0.5$ eV, yielding a spin moment of $0.55\mu_B$ per atom. Self-interaction corrections influence magnetism, by either removing it as in (b), or enhancing it as in (c). Magnetism is recovered in all cases under stretching. Bands crossing the Fermi level identify conductance channels in a long chain nanocontact: For increasing k-vector, all cases have six channels: (1±)$m_j = \pm 1/2(d_z^2 + s)$; (2±) $m_j = \pm 3/2(d_{xz}, d_{yz})$; (3±)$m_j = \pm 1/2(s + d_z^2)$. Depending on magnetization, additional d channels (4±) $m_j = \pm 3/2$, and (5-) $m_j = -5/2$ also cross Fermi.

larized, less massive ones conduct. The small spectator channel spin splittings are expected to have a negligible effect on transmission. As a result, conductance is poorly spin sensitive, and so is shot noise.

Experimental conductance and Fano factors are reasonably compatible with $\tau_{4\pm} = \tau_5 \sim 0$, and with e.g., $\tau_{1\pm} \sim 0.25$, $\tau_{2\pm} \sim 0.25$, $\tau_{3\pm} \sim 1$, or even better with $\tau_{1\pm} \sim 0.5$, $\tau_{2\pm} \sim 0$, $\tau_{3\pm} \sim 1$, restricting conductance in this case to the two channels that contain some *s* admixture. The latter hypothesis is particularly attractive, both because the large kinetic energy of *s* electrons naturally suggests a larger transmission despite low symmetry, and because in that two band case the shot noise will fall neatly on the two channel boundary, as noted for 18 experimental points.

6.6 CONCLUSION

It has been argued [24] that the zero bias anomalies observed in the differential conductance for Pt atomic chains provide evidence for local magnetic order. Indeed, the differential conductance often shows a pronounced structure near $V = 0$ (see figure (6.2)). However, this structure is very irregular and may have any sign or structure, which hampers a straight-forward interpretation. The shot noise measurement provides no direct evidence for magnetic order in the conductance channels for Pt atomic chains. Theoretical arguments however suggest that conductance and noise should involve only weakly polarized channels, where presence or absence of magnetism will make very little difference. A simple model where only two channels that contain *s* and *d* state admixture carry all the current is compatible with the data and the DFT calculations. Theoretically, it is found that safe predictions cannot be made about unstrained Pt chain magnetism without a proper correction, not yet available, of self-interaction errors in DFT. Yet, the strained Pt chains which are likely to dominate break junction histograms should theoretically be magnetic, and also possess a large orbital moment besides the spin moment. If any magnetic order is present for a consistent interpretation we would have to assume such moments would be formed by states that do not participate in the conductance.

In conclusion, we find strong evidence for an absence of strong magnetic order in the conductance channels for Pt atomic chains. The fact that this observation disagrees with many DFT-based computations suggests that effects beyond the present models, such as electron-electron correlations, may need to be considered. Some other tool will need to be devised to check whether this state of affairs is realized or not.

REFERENCES

[1] C. Untiedt, a. Yanson, R. Grande, G. Rubio-Bollinger, N. Agraït, S. Vieira, and J. van Ruitenbeek, *Calibration of the length of a chain of single gold atoms*, Physical Review B **66**, 1 (2002).

[2] A. I. Yanson, G. R. Bollinger, H. E. van den Brom, N. Agrait, and J. M. van Ruitenbeek, *Formation and manipulation of a metallic wire of single gold atoms*, Nature **395**, 783 (1998).

[3] K. T. Hideaki Ohnishi, Yukihito Kondo, *Quantized conductance through individual rows of suspended gold atoms*, Nature Physics **395**, 780 (1998).

[4] X. Liu, M. Bauer, H. Bertagnolli, E. Roduner, J. van Slageren, and F. Phillipp, *Structure and Magnetization of Small Monodisperse Platinum Clusters*, Phys. Rev. Lett. **97**, 253401 (2006).

[5] J. Dorantes-Dávila and G. M. Pastor, *Magnetic Anisotropy of One-Dimensional Nanostructures of Transition Metals*, Phys. Rev. Lett. **81**, 208 (1998).

[6] A. Delin and E. Tosatti, *Magnetic phenomena in 5d transition metal nanowires*, Phys. Rev. B **68**, 144434 (2003).

[7] J. Fernández-Rossier, D. Jacob, C. Untiedt, and J. J. Palacios, *Transport in magnetically ordered Pt nanocontacts*, Phys. Rev. B **72**, 224418 (2005).

[8] A. Smogunov, A. Dal Corso, and E. Tosatti, *Magnetic phenomena, spin-orbit effects, and Landauer conductance in Pt nanowire contacts: Density-functional theory calculations*, Phys. Rev. B **78**, 014423 (2008).

[9] A. Smogunov, A. D. Corso, A. Delin, R. Weht, and E. Tosatti, *Colossal magnetic anisotropy of monatomic free and deposited platinum nanowires*, Nature Nanotechnology **3**, 22 (2008).

[10] A. Thiess, Y. Mokrousov, S. Heinze, and S. Blügel, *Magnetically Hindered Chain Formation in Transition-Metal Break Junctions*, Phys. Rev. Lett. **103**, 217201 (2009).

[11] D. Djukic and J. M. van Ruitenbeek, *Shot noise measurements on a single molecule*, Nano Letters **6**, 789 (2006).

[12] N. Agraït, *Quantum properties of atomic-sized conductors*, Physics Reports **377**, 81 (2003).

[13] D. C. Ralph and R. A. Buhrman, *Observations of Kondo scattering without magnetic impurities: A point contact study of two-level tunneling systems in metals*, Phys. Rev. Lett. **69**, 2118 (1992).

[14] H. van den Brom and J. van Ruitenbeek, *Quantum Suppression of Shot Noise in Atom-Size Metallic Contacts*, Physical Review Letters **82**, 1526 (1999).

[15] S. K. Nielsen, M. Brandbyge, K. Hansen, K. Stokbro, J. M. van Ruitenbeek, and F. Besenbacher, *Current-Voltage Curves of Atomic-Sized Transition Metal Contacts: An Explanation of Why Au is Ohmic and Pt is Not*, Phys. Rev. Lett. **89**, 066804 (2002).

[16] J. Fernández-Rossier, D. Jacob, C. Untiedt, and J. J. Palacios, *Transport in magnetically ordered Pt nanocontacts*, Phys. Rev. B **72**, 224418 (2005).

[17] P. Roche, J. Ségala, D. C. Glattli, J. T. Nicholls, M. Pepper, A. C. Graham, K. J. Thomas, M. Y. Simmons, and D. A. Ritchie, *Fano Factor Reduction on the 0.7 Conductance Structure of a Ballistic One-Dimensional Wire*, Phys. Rev. Lett. **93**, 116602 (2004).

[18] L. DiCarlo, Y. Zhang, D. McClure, D. Reilly, C. Marcus, L. Pfeiffer, and K. West, *Shot-Noise Signatures of 0.7 Structure and Spin in a Quantum Point Contact*, Physical Review Letters **97**, 1 (2006).

[19] L. de la Vega, A. Martín-Rodero, A. L. Yeyati, and A. Saúl, *Different wavelength oscillations in the conductance of 5d metal atomic chains*, Phys. Rev. B **70**, 113107 (2004).

[20] F. Pauly, M. Dreher, J. Viljas, M. Häfner, J. Cuevas, and P. Nielaba, *Theoretical analysis of the conductance histograms and structural properties of Ag, Pt, and Ni nanocontacts*, Physical Review B **74**, 1 (2006).

[21] P. Lucignano, R. Mazzarello, A. Smogunov, M. Fabrizio, and E. Tosatti, *Kondo conductance in an atomic nanocontact from first principles*, Nature Materials **8**, 563 (2009).

[22] URL `http://www.pwscf.org`.

[23] M. Wierzbowska, A. Delin, and E. Tosatti, *Effect of electron correlations in Pd, Ni, and Co monowires*, Phys. Rev. B **72**, 035439 (2005).

[24] M. R. Calvo, Fernández-Rossier, Joaquín, Palacios, J. José, D. Jacob, Natelson, Douglas, and C. Untiedt, *The Kondo effect in ferromagnetic atomic contacts.*, Nature **458**, 1150 (2009).